Journal of Peptide Science, Vol. 2, 223–232 (1996)

Hydrophobic Effects on Antibacterial and Channel-forming Properties of Cecropin A–Melittin Hybrids

PADMAJA JUVVADI[1], SATYANARAYANA VUNNAM[1], ELIZABETH L. MERRIFIELD[1], HANS G. BOMAN[2] and R. B. MERRIFIELD[1]

[1] The Rockefeller University, New York, NY 10021, USA
[2] Department of Microbiology, University of Stockholm, Stockholm, Sweden

Received 10 January 1996
Accepted 23 January 1996

Abstract: The design of cecropin–melittin hybrid analogues is of interest due to the similarities in the structure of the antimicrobial peptides cecropin and melittin but differences in their lytic properties. We suspected that a hydrophobic residue in position 2 of milittin (Ile^8 in the hybrid) plays an important role in the activity of the 15-residue hybrid, KWKLFKKIGAVLKVL-NH_2, [CA(1–7)M(2–9)NH_2] and have now examined its role in the analogue toward five test bacteria. Deletion of Ile^8 reduced activity, and it was not restored by lengthening to 15 residues by addition of another threonine at the C-terminus. Replacement of Ile^8 by a hydrophobic leucine maintained good activity and Ala^8 was equally active for four organisms, although less active against *Staphylococcus aureus*. Replacement by the hydrophilic Ser^8 strongly reduced potency against all five organisms. Deletion of Leu^{15} decreased activity, but addition of Thr^{16} maintained good activity. The presence of hydrophobic residues appears to have a significant effect on the process of antibacterial activity. These peptide analogues showed voltage-dependent conductance changes and are capable of forming ion-pores in planar lipid bilayers. The antibacterial action of the peptides is thought to be first an ionic interaction with the anionic phosphate groups of the membrane followed by interaction with the hydrocarbon core of the membrane and subsequent reorientation into amphipathic α-helical peptides that form pores (ion-channels), which span the membrane. The analogue also showed an increase in α-helicity with an increase in hexafluoro 2-propanol concentration.

Keywords: Keywords: antimicrobial peptides; hydrophobic residue; ion-channels; pores; α-helix

INTRODUCTION

Cecropins are a major group of antibacterial peptides discovered in *Hyalophora cecropia*, which were later found in many other moths and in flies, as a response to the injection of live bacteria [1–3]. Peptide antibiotics constitute an important class of antibacterial molecules that is being rapidly expanded [4] owing to the development of resistance in pathogenic microorganisms to therapeutically useful antibiotics. The principal components in the cecropin family (cecropin A, B and D) are strongly homologous and are active against a variety of Gram-negative and Gram-positive bacteria. Cecropin A is synthesized as a preprocecropin precursor and processed *in vivo* to give a linear 37-residue peptide [5]. Synthesis and studies, first with cecropin A (1–33) [6], followed by cecropin A [7] and a series of analogues with altered N-termini [8], showed the importance of an amphipathic helix. Other medium sized peptides such as β-endorphins also revealed the amphipathic helix [9] as a structural determinant for activity [10]. The secondary structure of cecropin was predicted to have a helix–bend–helix motif from sequence analy-

Abbreviations: CA, cecropin A; CD, circular dichroism; 2D-NMR, two-dimensional nuclear magnetic resonance; DIEA, *N,N*-diisopropylethylamine; HEPES, *N*-(2-hydroxyethyl)piperazine-*N'*-(2-ethanesulfonic acid); HFIP, hexafluoro 2-propanol; LC, lethal concentration; M, melittin; $[Phy]_2$PtdCho, diphytanoyl phosphatidylcholine; PtdSer, phosphatidyl serine.

Address for correspondence: Prof. R. B. Merrifield, The Rockefeller University, 1230 York Ave, New York, NY 10021, Tel: 212-327-8244; Fax: 212-327-7974.

CCC 1075-2617/96/040223-10

sis and circular dichroism (CD) measurements [6, 11]. This was confirmed for cecropin A in a low polarity solvent by 2D-NMR studies [12].

The peptides are amphipathic and highly helical in the presence of organic solvents and also when in contact with a lipid bilayer. Several molecules aggregate to form a pore or channel that spans the bilayer [13] and the N-terminal segment was found to be an essential requirement for antibacterial action [14]. A comparable range of susceptible pathogens is observed with melittin, a 26-residue toxic peptide (Table 1) isolated from bee venom [15], with basic and hydrophobic segments like cecropin but arranged in opposite order. Melittin is also amphipathic [16] and exhibits antibacterial activity [17], but has the very detrimental property of being strongly haemolytic and toxic to eukaryotic cells [18]. Interestingly, reversal of melittin segments as in M(16–26)M(1–13)NH_2 [19] gave an active peptide that did not lyse red cells.

Our interest in the design and synthesis of chimeric peptides that are cecropin–melittin hybrids is mainly due to the similarities in structure of these two peptides but differences in their lytic properties. In addition, two hybrids tested were also active against the malarial parasite *Plasmodium falciparum* [19]. With the aim of finding potent antibacterial peptides we have designed and synthesized various hybrid peptides from the N-terminal segments of cecropin A and melittin with enhanced antimicrobial activity [7, 8, 20]. The problem of identifying optimal structural requirements for activity was further examined with the aid of a series of model peptides [21], and the retro sequences [22]. To determine the minimum size of cecropin analogues that was actually needed for activity we synthesized several shortened cecropin A–melittin hybrids with as few as 15 residues (60% size reduction relative to cecropin A) [23]. These hybrid analogues were more potent with respect to the parental peptide cecropin A and interestingly did not retain the cytotoxic character of melittin. More recently the hybrid peptide with 12 residues in length CA(1–7)M(5–9)NH_2 was found to have high antibacterial activity. Further reduction in size led to inactive analogues [23].

Loss of antimicrobial activity in the analogue obtained by replacement of Ile^8 by Pro^8 in cecropin A [24], led us to study the important role of Ile^8 (position 2 of the melittin segment) in the antibacterial activity of the hybrid peptide analogues. Therefore we synthesized various short cecropin A–melittin hybrid analogues (Table 1) to understand the role of a hydrophobic residue at position 8 in the antimicrobial action of these peptide molecules The pore-forming ability and the voltage-dependent conductance of these analogues was also studied.

MATERIALS AND METHODS

Synthesis and Purification of the Peptides

All the peptides were synthesized by the solid-phase peptide synthesis technique [25]. They were prepared on *p*-methyl benzhydrylamine resin [26] (0.64–0.76 mmol per g) (Peptide International, Louisville, KY) either manually by our most effective methods [6] or on an Applied Biosystems model 430A synthesizer. Protected amino acids were obtained from Peninsula

Table 1 Primary Structures of Cecropin A–Melittin Hybrid Analogues

Peptide amide	No. of residues	Amino acid sequence	
Cecropin A (CA)	37	KWKLFKKIEKVGQNIRDGII KAGPAVAVVGQATQIAK	
Melittin (M)	26	GIGAVLKVLTTGLPALISWI KRKRQQ	
Hybrid analogues		1 (CA) 7	2 (M) 10
1 CA(1–7)M(2–9)	15	KWKLFKK	IGAVLKVL
2 CA(1–7)M(2–8)	14	KWKLFKK	IGAVLKV
3 CA(1–7)M(2–10)	16	KWKLFKK	IGAVLKVLT
4 CA(1–7)M(3–9)	14	KWKLFKK	GAVLKVL
5 CA(1–7)M(3–10)	15	KWKLFKK	GAVLKVLT
6 CA(1–7) [L^2]M(2–9)	15	KWKLFKK	LGAVLKVL
7 CA(1–7) [A^2]M(2–9)	15	KWKLFKK	AGAVLKVL
8 CA(1–7) [S^2]M(2–9)	15	KWKLFKK	SGAVLKVL

Laboratories (Belmont, CA), The couplings, with dicyclohexylcarbodiimide in dichloromethane, or symmetrical anhydrides in dimethylformamide (DMF), or HOBt esters in DMF, were monitored by the quantitative ninhydrin method [27]. The *tert*-butoxycarbonyl (Boc) group was used for temporary N^{α}-protection of amino acids, and more acid stable groups (2-chlorobenzyloxy carbonyl for Lys and formyl for Trp) were used for side-chain protection. The N^{α}-Boc was removed at each cycle and from the completed peptide-resin by 50% trifluoroacetic acid (TFA) in methylene chloride. The N^{in}-formyl protecting group of tryptophan was removed by reacting twice for 1 min each with 50% piperidine in DMF, and the peptide was cleaved from the resin using either high or low/high HF procedures [28].

Peptides were purified by a two-step procdure: gel filtration on a 2.4 × 90 cm column of Sephadex G-25 (Pharmacia LKB, Piscataway, NJ), eluted with 1 M AcOH at 45 ml/h, followed by reverse-phase preparative HPLC on a 2.2 × 25 cm C-18 Vydac column (15–20 μm, 300 Å pores, the Separations Group, Hesperia, CA) using a linear gradient of 10–60% acetonitrile in water containing 0.05% TFA at a rate of 20 ml/min. the eluent was monitored at 220 nm on a Kratos Spectroflow 757 absorbance detector. The main peak was assessed for homogeneity by analytical HPLC with a reverse-phase column, 0.46 × 25 cm, packed with 5 μm C-18 silica beads, and the composition determined by amino acid analysis. Hydrolysis of free peptides was done with 6N HCl in evacuated, sealed tubes at 110 °C, 18 h and the peptide resins were hydrolysed in 12N HCl/propionic acid (1:1 v/v) at 130 °C, 15 h [29]. The homogeneity and the molecular weight of the purified peptide was determined by electrospray mass spectrometry [30].

Antibacterial and Erythrocyte Lysis Assays

Thin agar plates were prepared with 6 ml of rich medium containing 1–4 × 10^5 colony-forming units of the respective log-phase test bacteria [31]. Wells of 3 mm diameter were punched in the plates, and for each peptide and each test bacterium, 3 μl aliquots of a series of peptide dilutions were placed in the small wells. The concentration of each peptide was determined from its absorbance at 280 nm ($\varepsilon = 5.6 \times 10^3\,cm^{-1}\,M^{-1}$). Plates were incubated overnight at 38 °C, the diameters of the zones of inhibition measured and the lethal concentration (LC), the lowest concentration that completely inhibits growth, was calculated as described [32].

An erythrocyte lysis assay was adapted from the antibacterial plate assay. The plates contained 6 ml of 1% agarose, 0.9% NaCl and 10% sheep erythrocytes suspended in Alsever's solution. The dilution series of the peptide was placed in the wells. After the incubation at 38 °C for 20 h, the diameters of the clear zones were recorded and the LC values calculated as before [32]. The LC is the lowest concentration of peptide in which the diameter of the clear zone is no larger than the sample well. This is determined by extrapolation of the square of the zone diameter against the log of the peptide concentration.

Circular Dichroism Analyses

CD spectra were recorded in an Aviv 62DS spectropolarimeter. Peptides (final concentration of 25 μM) were dissolved in 2.5 mM sodium phosphate buffer, pH 7.4, containing 0–20% (v/v) hexafluoro 2-propanol (HFIP). Five consecutive 250–190 nm scans were made in a 1 mm path length cell at 22–25 °C. The data were averaged and analysed by the prosec program [33] to determine the percentage of α-helix, β-sheet, β-turn and random coil.

Electrical Conductivity Measurements

The equipment and procedures were similar to those described previously [13, 34]. Bilayers of Mueller–Rudin type [35] were formed from lipids (15 mg/ml) consisting of 75% diphytanoyl phosphatidyl choline ($[Phy]_2$PtdCho) and 25% phosphatidyl serine (PhtSer) (both from Avanti Polar Lipds, Pelham, AL) across a 0.5 mm diameter hole in a teflon septum separating two half cells of 1.5 ml volume each. The entire cell assembly was washed with 30% methanol and sonicated each time prior to use. To each half cell was added 1.5 ml solution of 0.1 M NaCl/10 mM HEPES, pH 7.1–7.4. The hole was pretreated with 0.2 μg of $[Phy]_2$PtdCho dissolved in 0.2 μl of hexane to each side, and the organic solvent was evaporated. The cell was fixed in the cell holder, and KCl-saturated calomel electrodes (Ingold, Wilmington, MA) connected the aqueous compartments to the measuring circuit. The mixture of lipids dissolved in one of the organic solvents (decane, hexadecane or squalene, Aldrich, Milwaukee, WI, gold label) were applied across the hole with a fine brush or a pipette. On standing for a few minutes the solvent diffused out and the lipid self-organized into a black lipid bilayer. Bilayer formation was followed by an increase in capacitance. The rear compartment (*trans*)

was held at ground and voltage was applied to the front (*cis*) compartment. Current measurements were performed with a home-built current-to-voltage converter (based on a Zeltex 133 operational amplifier) with a feedback resistance of 10^9 ohms and a feedback capacitance between 10 and 300 pF, yielding cutoff frequencies between 3 and 100 Hz. The amplifier output was recorded on a chart recorder (series 4900 super scribe, Houston Instruments, Austin, TX) and was observed simultaneously on a Biomation 802 transient recorder (Gould, Santa Clara, CA).

The membrane thickness was estimated from its measured capacitance using the relation $d = \varepsilon A/C$, where d is the thickness of the bilayer in Å, ε is the dielectric constant of the lipid, A is the area of bilayer in mm^2 and the C is the capacitance in faradays. The basic conductance of the bilayer was recorded for at least 15 min. The conductance did not exceed 0.02 nS and no channel activity was observed. The peptides at 30–4000 ng/ml concentrations were dissolved in water and added to the *cis* compartment at 0 mV, an equal volume of water was added to the *trans* compartment. They were allowed to equilibrate for at least 30 min. A potential of -70 mV was applied until the pore activity was observed, and then the voltage was varied from negative to positive values. The voltage was applied for enough time (~ 10 min) to collect signals from pores opening and closing.

RESULTS

The primary structures of cecropin A–melittin hybrid analogues reported here are depicted in Table 1, along with parent cecropin A and melittin for comparison. All peptides were prepared as C-terminal amides by the solid-phase technique using Boc/benzyl chemistry, cleaved with HF, and were purified on Sephadex G-25 followed by reverse-phase chromatography in satisfactory yields (38–46% overall yield). All synthetic peptides had the expected amino acid composition by amino acid anlaysis (± approximately 3%) and the correct molecular weights determined by electrospray mass spectrometry (precision ± 0.3 mass unit) [30]. The antibiotic and haemolytic activities of these analogues were measured by inhibition zone assays from which the lethal concentrations were derived (Table 2). A good correlation was found between the assays performed independently in two of our separate laboratories at New York and Stockholm.

Replacement of Ile^8 by Pro^8 in cecropin A [24] reduced the activity and the observed helicity, and a correlation was made between the loss of helicity and decrease in antibacterial activity in a series of peptides. Our present investigation is aimed at understanding the role of a hydrophobic residue at position 8 in short cecropin–melittin hybrid analogues. Deletion of Ile^8 as in CA(1–7)M(3–9)NH_2 **(4)** decreased activity, while retention of Ile^8 and addition of Thr^{16} **(3)** maintained good activity (Table 2). In order to further investigate the role of Ile^8 in CA(1–7)M(2–9)NH_2 **(1)**, it was replaced with hydrophilic Ser, **(8)**, and hydrophobic Leu, **(6)**, or Ala, **(7)**, (Table 1).

Antimicrobial Activity

Deletion of Leu^{15}, CA(1–7)M(2–8)NH_2 **(2)** (Table 1) reduced the activity (3 to 16-fold) against *Escherichia coli*, *Staphylococcus aureus* and *Bacillus subtilis* (Table 2) when compared with CA(1–7)M(2–9)NH_2 **(1)**, while addition of Thr^{16} in CA(1–7)M(2–10)NH_2 **(3)** significantly enhanced the activity against *Staph. aureus* (Table 2). In order to understand the sig-

Table 2 Lethal and Lysis Concentrations (μM) for Cecropin A–Melittin Hybrids[a]

Peptide amide	Size	D21	OT 97	BS 11	Sp 1	Sac 1	SRC
1 CA(1–7)M(2–9)	15	1.0	4.0	0.5	0.3	4.0	>300
2 CA(1–7)M(2–8)	14	8.6	7.5	8.0	0.5	14.8	>280
3 CA(1–7)M(2–10)	16	1.4	3.7	2.7	1.1	0.9	>400
4 CA(1–7)M(3–9)	14	3.9	14	10	0.9	2.9	>320
5 CA(1–7)M(3–10)	15	9.1	14	6.3	1.2	>200	>600
6 CA(1–7) [L^2]M(2–9)	15	1.6	4.5	7.5	0.8	0.9	>360
7 CA(1–7) [A^2]M(2–9)	15	1.5	3.5	5.2	0.5	13.5	>200
8 CA(1–7) [S^2]M(2–9)	15	9.7	6.2	28.6	17.8	89.2	>300

[a] Lethal concentrations calculated from inhibition zones on agarose plates seeded with the respective organisms: D 21 = *Escherichia coli*; OT 97 = *Pseudomonas aeruginosa*; Bs 11 = *Bacillus subtilis*; SP 1 = *Streptococus pyogenes*; Sac 1 = *Staphylococcus aureus* strain cowan 1; SRC = sheep red cells.

nificance of a hydrophobic residue and rule out the possible contribution of the chain length, analogue **5** was synthesized by deletion of Ile^8 and lengthening the chain by addition of Thr^{16} at the C-terminus of CA(1–7)M(2–9)NH_2. The resulting analogue, CA(1–7)M(3–10)NH_2 (**5**), was generally less potent than CA(1–7)M(2–9)NH_2 (23) and against *Staph. aureus* (LC > 200 μM) it was much less potent, which further documents the selective effects of cell membrane composition on the antimicrobial activity of peptides.

Replacement of Ile^8 by the hydrophilic residue, Ser^8 (Table 2), showed strong reduction in the activity against all the bacteria tested. The presence of either Ile^8 or Leu^8 at position 8 maintained equal activity with two Gram-negative and one Gram-positive test bacteria (Table 2) but the two other Gram-positive bacteria **1** and **6** showed opposite effects. CA(1–7)M(2–9)NH_2 (**1**), containing Ile^8 (LC = 0.5 μM), is 15-fold more active on *B. subtilis* than peptide **6** containing Leu^8 (LC = 7.5 μM). However, analogue **6** possesses significantly enhanced activity against *Staph. aureus* (LC = 0.9 μM) when compared with **1** (LC = 4 μM). Replacement of Ile^8 with Ala^8 in **7** decreased the activity against *Staph. aureus* and *B. subtilis* but did not affect the activity against other test bacteria (Table 2).

Peptide Conformation

Peptide CA(1–7)M(2–8)NH_2 (**2**) and CA(1–7)M(3–9)NH_2 (**4**), in 2.5 mM sodium phosphate buffer showed significant levels of β-sheet conformation. With CA(1–7)M(3–9)NH_2 the helix content rose to 69% at 16–20% hexafluoro 2-propanol (HFIP), while CA(1–7)M(2–8)NH_2 showed a lower tendency to adopt an α-helix structure, 49% α-helix at 20% HFIP (Table 3). The other six analogues had no defined structure in the absence of HFIP, but a tendency to adopt an α-helix structure was observed at 8% HFIP which was more prevalent at higher HFIP concentrations (Table 3). Two analogues CA(1–7)M(2–10)NH_2 (**3**) and CA(1–7) [L^2]M(2–9)NH_2 (**6**), showed significant α-helix structure, 11% and 24% respectively in 2.5 mM sodium phosphate buffer, which increased with increasing concentrations of HFIP. The tendency of these two peptides to aggregate may account for some loss of helicity at 20% HFIP.

Electrical Conductivity

In order to study the ability of the short cecropin–melittin hybrid analogues to form ion-channels and disrupt membranes, electrical conductivity measurements, showing the channel activity of these peptides, was examined in artificial lipid bilayers. Lipid membranes formed across a small hole in a Teflon partition have a relatively large area and thus a high capacitance [36].

Analogue **1**, CA(1–7)M(2–9)NH_2 (0.1 μM), showed an average pore conductance of 0.5 ± 0.07 nS and a maximum conductance of 1.1 nS (Table 4). CA(1–7)M(2–10)NH_2 (**3**), produced currents with definite channel openings and closings (Figure 1) at a concentration of 0.05 μM. Our attempts to measure a change in conductance with analogue **5**, CA(1–7)M(3–10)NH_2, and a 14-residue analogue CA(1–7)M(2–8)NH_2 (**2**), over a time range of 6 h were unsuccessful. These chimeric peptides did not induce channel activity or conductivity increase though the peptide concentration was slowly increased from 0.05 μM to as high as 2.6 μM (for analogue **5**) and 2.3 μM (for analogue **2**) at regular intervals of time (Table 4). These two analogues did not show channel activity even with the lipid

Table 3 Percentages of α-helix, β-sheet and Random Coil in Cecropin A-Melittin Hybrids[a]

Peptide amide	0% HFIP			4% HFIP			8% HFIP			12% HFIP			16% HFIP			20% HFIP		
	α	β	r	α	β	r	α	β	r	α	β	r	α	β	r	α	β	r
1 CA(1–7)M(2–9)	0	0	69	0	8	62	28	63	9	91	0	9	100	0	0	100	0	0
2 CA(1–7)M(2–8)	6	20	74	7	68	25	25	55	20	34	46	20	51	46	3	49	49	2
3 CA(1–7)M(2–10)	11	0	68	45	0	37	59	7	34	89	0	11	97	0	3	88	0	12
4 CA(1–7)M(3–9)	2	16	67	8	25	56	33	18	49	64	0	36	68	0	32	69	0	31
5 CA(1–7)M(3–10)	0	0	65	0	11	59	0	44	45	63	0	37	91	0	9	100	0	0
6 CA(1–7) [L^2]M(2–9)	24	0	57	68	0	21	53	0	29	59	0	25	70	0	22	63	0	36
7 CA(1–7) [A^2]M(2–9)	0	0	87	4	0	93	60	0	40	100	0	0	100	0	0	100	0	0
8 CA(1–7) [S^2]M(2–9)	0	0	94	0	0	100	50	0	50	100	0	0	100	0	0	100	0	0

[a] Calculated from circular dichroism measurements.

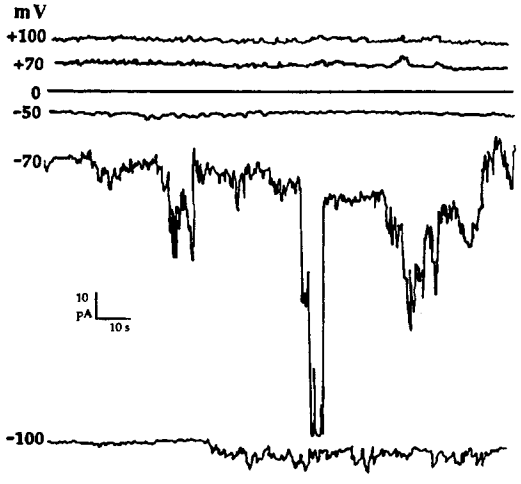

Figure 1 Demonstration of pore activity of CA(1–7)M-2–10)NH_2 (**3**), 0.05 μM on the *cis* side of PtdSer/$[Phy]_2$Ptd-Cho bilayer, at different applied voltage (mV).

membranes as thin as 16 Å. Overall the system was found to be stationary for the duration of the recording and showed that there was no increase in the current flowing through the bilayer with time.

In order for a short peptide to span the membrane and form channels, the thickness of the bilayer formed by using the lipid solution in squalene or haxadecane was appropriate. The capacitance, thickness and composition of the bilayer vary as a function of hydrocarbon solvent used in their formation [37]. The thickness of the artificial lipid membrane in Å was estimated from the capacitance measured in faradays, with the dielectric constant of 2.8 and the area of the bilayer measured in mm^2. From several measurements the thicknesses of the bilayers formed in squalene and in hexadecane were calculated as 16–24 Å and 22–28 Å respectively. These distances were found to be adequate for these 14 and 15-mers to span the membrane (1.5 Å × 15 = 22.5 Å). When the bilayers were formed in decane the calculated thickness was 30–38 Å, which is approximately the length of the two polar phospholipid hydrocarbon chains. These peptides showed similar channel behavior with the bilayers formed from lipids in both hexadecane and squalene.

In the experiment with analogue **3**, CA(1–7)M(2–10)NH_2, the maximum pore conductance was very large, corresponding to an ion flow of roughly 1×10^7 to 6×10^8 ions per second at − 70 mV. The large ion flow is possibly due to the multiple conductance levels formed by the simultaneous presence of pores, but the quantitative determination of number of channels and conductance levels in each pore was not possible. The minimum conductance observable was ~0.02 nS while the maximum went as high as 1.4 nS. The average channel conductance observed for CA(1–7)M(2–10)NH_2 (**3**) was 0.5 ± 0.06 nS at an applied voltage of − 70 mV. The optimum peptide concentration required for the pore activity in this case was 0.05 μM (Table 4). Reversal of the voltage source to positive on the peptide side caused the current to reverse and then to increase linearly within a few minutes (~20 min). The steady state of conductance was observed with time but no channels were noticed (Figure 1). Switching back to the negative voltage led to the formation of fluctuations or pores. Over the time scale of the experiment

Table 4 Channel (G_l) and Macroscopic (G_m) Conductances[a] Induced by Short Cecropin A–Melittin Hybrid Analogues on Planar Lipid Bilayers

Peptide amide	Conc.[b] (μM)	G_l (nS)	G_m (nS)	G_m/Conc. (nS/μM)	Biological activity
1 CA(1–7)M(2–9)	0.1	0.5 ± 0.07	1.1	11.0	Highly active
2 CA(1–7)M(2–8)	2.3	None[c] < 0.02	None[c] < 0.02	≪ 0.009	Less active
3 CA(1–7)M(2–10)	0.05	0.5 ± 0.06	1.4	28.0	Highly active
5 CA(1–7)M(3–10)	2.6	None[c] < 0.02	None[c] < 0.02	≪ 0.008	Less active
6 CA(1–7) [L^2]M(2–9)	0.3	0.25 ± 0.04	1.2	4.0	Highly active
8 CA(1–7) [S^2]M(2–9)	2.7	None[c] < 0.02	None[c] < 0.02	≪ 0.007	Less active

[a] Macroscopic conductance is the maximum conductance observed at the given peptide concentration.
[b] Concentrations necessary for optimum channel activity.
[c] No channels observed. A conductivity of < 0.02 nS could have been seen.

the peptide channels in the membrane were constant. Analogue **3** was found fo be a very good example of rectification.

A decrease in potential from −70 to −50 mV in analogue **3**, did not induce any conductance or channel formation (Figure 1), and an increase from −70 to −100 mV also did not correspondingly increase the pore formation. At −100 mV there was an increase in the open time of the channels to ~80 s, as compared to those open for approximately 30 s at −70 mV. However, the conductance observed from the channels open for a long time did not exceed ~0.02 nS. For this peptide a cricial voltage appears to be necessary to obtain an observable open channel. The electric field is apparently involved in conformational changes of the peptide channel aggregate.

In the case of the other three analogues studied, **1** with Ile^8, **6** with Leu^8, and **8** with Ser^8, large variations were recorded. Analog **1**, CA(1–7)M(2–9)NH_2 (0.1 μM), showed an average pore conductance of 0.5 ± 0.07 nS and the maximum conductance of 1.1 nS (Table 4), and is comparable with the channel activity of analogue **6** (0.3 μM). Analogue **6**, CA(1–7)[L^2]M(2–9)NH_2, induced channel activity at a concentration of 0.1 μM though the conductance observed was only ~0.02 nS or less. After recording for an hour without any significant increase in pore conductance the concentration of the peptide was increased to 0.3 μM, resulting in a large increase in the level of channel activity and pore conductance. Multiple pore conductance levels were observed (Figure 2), which are probably due to the simultaneous presence of several small open channels within the bilayer. The average pore conductance was approximately 0.25 ± 0.04 nS (Table 4) and the large conductance showed an enormous ion flow of 4×10^6–5×10^8 ions per second at −70 mV. The minimum conductance observable was ~0.02 nS, even at 0 mV which may be considered as ground

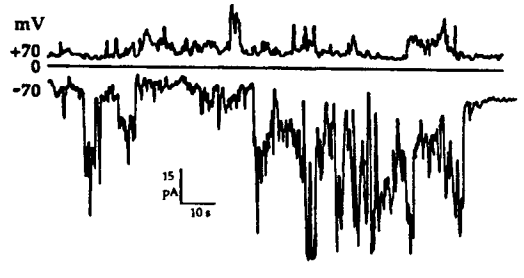

Figure 2 Current response of CA(1–7) [L^2]M(2–9)NH_2 (**6**), 0.3 μM on the *cis* side of PtdSer/[Phy]$_2$PtdCho bilayer, at applied voltage (mV).

level noise, while the maximum conductance recorded was 1.2 nS. After further increasing the peptide concentration to 0.5 μM, the level of activity was high, non-stationary and rapid, resulting in disruption of the membrane, presumably due to large bursts of ions lysing the membrane. It was possible to observe a regular and stable ion-channel formation only in a narrow range of CA(1–7) [L^2]M(2–9)NH_2 (**6**) concentrations.

Reversing the voltage source to positive on the peptide side with CA(1–7) [L^2]M(2–9)NH_2 (**6**) showed fewer (10-fold) pores compared with those observed at negative voltage on the peptide side (Figure 2) revealing the voltage dependent behaviour of the macroscopic current for analogue **6**. Similar experiments carried out with CA(1–7) [S^2]M(2–9)NH_2 (**8**) did not induce conductance increase or channel activity with the bilayer formed in squalene (thickness estimated to be 18 Å). Increasing the concentration of the peptide to 2.7 μM (9-fold) as compared to the concentration of analogue **6** (0.3 μM), and analogue **1** (0.1 μM) or reducing the thickness of the lipid membrane did not induce conductance or channel activity over a period of 6–8 h.

DISCUSSION

Studies on cecropin–melittin hybrid analogues showed that a hydrophobic residue at position 8 made a significant contribution to their function, suggesting a possible apolar interaction with the artificial lipid bilayer and, probably, the bacterial membrane with the amino acid at position 8 of the peptide molecule. The effect was seen with all the test bacteria, but *Staphylococcus aureus* was found to be more selective. Analogues **1** (Ile^8) and **7** (Ala^8) showed a significantly lower activity against *Staph. aureus* than analogue **6** (Leu^8), possibly due to the differences in hydrophobicities. The hydrophobicity and α-helical propensity of an amino acid side chain are not correlated with each other, but each contributes to the stability of the amphipathic α-helix [38]. The direct evaluation of the hydropathy may be related to the ensemble average of the side chain to prefer the interior to the exterior of the peptide, which in turn may be correlated with the activity. It is reasonable to assign a lower, but necessary, hydrophobic force to the peptide containing Leu as compared to those possessing Ile and Ala, from the water-vapour transfer free energies (Ile: 4.4; Ala: 3.9; Leu: 4.5) [39] and the interior–exterior distribution of amino acid side chains (Ile: 4.5; Ala: 5.3; Leu: 3.2) [40].

These differences in responses encountered indicate that a single unique mechanism is not common to all bacteria for interaction of antimicrobial peptide, and *Staph. aureus* appears to be more selective when compared with other organisms.

CA(1–7)M(2–9)NH_2 (**1**) with Ile^8, CA(1–7)M(2–10)NH_2 (**3**) and CA(1–7) [L^2]M(2–9)NH_2 (**6**) with Leu^8 showed high antibacterial activity against both Gram-positive and Gram-negative bacteria, while analogue **2**, CA(1–7)M(2–8)NH_2 (lacking Leu^{15} and CA(1–7) [S^2]M(2–9)NH_2 (**8**) with Ser^8, were less active against all the test bacteria (Table 2). None of the analogues tested lysed red blood cells. These results demonstrate the specificity of activity of the cecropin–melittin hybrids only for bacteria and not for eukaryotic cells.

The helical content of analogue **2**, [CA(1–7)M(2–8)NH_2] which is $< 50\%$ even at 20% HFIP, a structure-inducing solvent, correlates with its low activity against all the test bacteria (Table 2). Analogues CA(1–7)M(2–10)NH_2 (**3**) and CA(1–7) [L^2]M(2–9)NH_2 (**6**) showed a significant α-helix structure even at 0% HFIP (Table 3), which may be correlated with their high activity (Table 2) and channel-forming ability (Table 4). The length of the peptide analogue **2** may be too short to span the membrane and the weakened helical character could have decreased the ability to induce channels in bilayers (Table 4), while the helix stability of analogues **3** and **6** correlates with their channel-forming ability.

In aqueous organic solvents and lipids the short cecropin–melittin hybrid analogues are found to be helical. The helices are thought to form transmembrane ion-channels by aggregating in bundles with their hydrophilic residues on the inside, making a water-filled pore, and their hydrophobic residues on the outside, interacting with the hydrocarbon chains of the lipid. The membrane has a very non-homogeneous environment with a high density of polar head groups, at the interface between the thin hydrocarbon core and the aqueous solvent imposing strong constraints on the favourable peptide conformations that interact and span the membrane. The length of the α-helix of a 15-residue analogue may approximately be calculated as 22.5 Å (15-residue × 1.5 Å/residue), which is rather insufficient to span the thickness of the hydrophobic region of the phospholipid bilayer formed in decane solvent (measured as 30–38 Å). These analogues did not show either conductance increase or ion-channel formation in bilayers formed in decane. The thickness of the bilayer formed in squalene or hexadecane was of appropriate length for the short analogues to span the hydrophobic stretch of the membrane, suggesting amphipathic helical peptides are structural and functional entities by themselves. The lipid bilayers and the cell membranes are chiral and it was generally assumed that specific chiral interactions of the peptide are essential for the activity. However, our earlier study with D-peptide analogues suggested no stereo-selective interaction with a chiral receptor or lipid [41, 42], but only self-interactions to form membrane-spanning structures.

Peptide analogues (**1**, **3** and **6**) were effective pore formers, while analogues **2**, **5**, and **8** did not induce channels and increase conductance in artificial lipid membranes. The precise sequence of residues is generally not critical for channel formation as long as the peptide is amphipathic, long enough and capable of forming hydrophobic interactions with the bilayer so as to stabilize the channel aggregate. A variety of interactions of peptides with lipid membranes is possible. Insertion of a hydrophobic helix into a membrane is thermodynamically favourable with a stabilization energy of 15 kcal/mol [43]. The voltage sensing may result from the interaction between the dipole formed from the amino acid backbone and the electrical field across the membrane [44]. These short analogues are thought to have first an ionic interaction with the anionic phosphate groups of membrane followed by hydrophobic interactions involving the amino acid residue at the eighth position with the hydrocarbon core of the membrane and subsequent reorientation into amphipathic α-helical peptides that form pores (ion-channels). To our knowledge, there is no direct experimental evidence to simultaneously elucidate the orientation of the peptide at the membrane interface, the mechanism of interaction with the bilayer and the peptide conformational preferences in membranes.

The frequency of channel activity correlated with the concentration of the peptide and showed regular and stable channel activity at a particular concentration, while higher concentrations led to large pores destabilizing the membrane and resulting in its disruption. The different levels of multistate conductance observed were not the integral multiples of a unit conductance, which implies that there are different states of the pores formed due to the different sized aggregates. The concentration of the peptide in the membrane eventually reaches a point causing an increase in the membrane potential, as observed for melittin [45], and disrupting the lipid organization, which leads to lysis. The strong concentration dependence of frequency of channel for-

mation may reflect the necessity of relatively large numbers of molecules to form functional channels. This behavior is comparable to that of alamethecin [46] and its synthetic analogue [47]. The membrane was stable for more than 8 h when the optimum peptide concentration was employed. Therefore, these results show that the disruption of membranes by high voltage is not due to a simple detergent effect.

Comparison of the activity with the structure and conformation of these short peptides emphasizes the presence of hydrophobic residues as an important factor for the antibacterial activity in addition to the amphipathicity of the analogues. The thickness of the bilayer could be varied as a function of different organic solvents owing to the difference in the capacity of organic solvents to promote interdigitation of lipids. The calculated length of the α-helix of 15-residue analogues matches the hydrocarbon thickness of lipid bilayers made under certain conditions and facilitates ion-channel formation. Interestingly the presence of a hydrophobic residue at position 8, and the helical nature of these short cecropin A–melittin hybrid analogues also facilitated voltage-dependent conductance changes and enhanced their channel-forming ability.

Acknowledgements

This work was supported by US Public Health Service Grant DK 01260, and Swedish Natural Science Research Council Grant B-BU 2453. We are grateful to Prof. David Mauzerall (Head, Laboratory of Photobiology, The Rockefeller University) for helpful discussions and also for the use of the electrical conductance equipment. We thank Prof. Brian Chait (Director of the Mass Spectrometric Biotechnology Research Resource of the Rockefeller University) for the mass spectral analyses.

REFERENCES

1. H. Steiner, D. Hultmark, A. Engstrom, H. Bennich and H. G. Boman (1981). Sequence and specificity of two antibacterial proteins involved in insect immunity. *Nature 292*, 246–248.
2. H. G. Boman and D. Hultmark (1987). Cell-free immunity in insects. *Annu. Rev. Microbiol. 41*, 103–126.
3. H. G. Boman in: *Phylogenetic Perspectives in Immunity: The Insect-Host Defense*. J. Hoffmann, S. Natori and C. Janeway, Eds., p. 24–37, R. G. Landes Biomedical Publishers, Texas 1994.
4. H. G. Boman (1995). Peptide antibiotics and their role in innate immunity. *Annu. Rev. Immunol. 13*, 61–92.
5. H. G. Boman, I. A. Boman, D. Andreu, Z-Qu. Li, R. B. Merrifield, G. Schlenstedt and R. Zimmermann (1989). Chemical synthesis and enzyme processing of precursor forms of cecropin A and B. *J. Biol. Chem. 264*, 5852–5860.
6. R. B. Merrifield, L. D. Vizioli and H. G. Boman (1982). Synthesis of the antibacterial peptide cecropin A (1–33). *Biochemistry 21*, 5020–5031.
7. D. Andreu, R. B. Merrifield, H. Steiner and H. G. Boman (1983). Solid-phase synthesis of cecropin and related peptides. *Proc. Natl. Acad. Sci. USA 80*, 6475–6479.
8. D. Andreu, R. B. Merrifield, H. Steiner and H. G. Boman (1985). N-terminal analogues of cecropin A: Synthesis, antibacterial activity and conformational properties. *Biochemistry 24*, 1683–1688.
9. J. P. Segrest, R. L. Jackson, J. P. Morrisett and A. M. Jr. Gotto (1974). A molecular theory of lipid–protein interactions in the plasma lipo proteins. *FEBS Lett. 38*, 247–253.
10. E. T. Kaiser and F. J. Kezdy (1983). Secondary structures of proteins and peptides in amphiphilic environments. *Proc. Natl. Acad. Sci. USA 80*, 1137–1143.
11. H. Steiner (1982). Secondary structure of the cecropins: antibacterial peptides from the moth *Hyalophora cecropia*. *FEBS Lett. 137*, 283–287.
12. T. A. Holak, A. Engstrom, P. J. Kraulis, G. Lindeberg, H. Bennich, T. A. Jones, A. M. Gronenborn and G. M. Clore (1988). The solution conformation of the antibacterial peptide cecropin A: a nuclear magnetic resonance and dynamical simulated annealing study. *Biochemistry 27*, 7620–7629.
13. B. Christensen, J. Fink, R. B. Merrifield and D. Mauzerall (1988). Channel-forming properties of cecropins and related model compounds incorporated into planar lipid membranes. *Proc. Natl. Acad. Sci. USA 85*, 5072–5076.
14. J. Fink, R. B. Merrifield, A. Boman and H. G. Boman (1989). The chemical synthesis of cecropin D and an analog with enhanced antibacterial activity. *J. Biol Chem. 264*, 6260–6267.
15. E. Habermann and J. Jentsch (1967). Sequence analysis of melittin from tryptic and peptic degradation. *Hoppe-Seylers Z. Physiol. Chem. 348*, 37–50.
16. T. C. Terwilliger and D. Eisenberg (1982). The structure of melittin. II. Interpretation of the structure. *J. Biol. Chem. 257*, 6016–6022.
17. H. G. Boman (1982). Humoral immunity in insects and the counter defense of some pathogens. *Fortschr. Zool. 27*, 211–222.
18. E. Habermann (1972). Bee and wasp venoms. *Science 177*, 314–322.
19. H. G. Boman, D. Wade, I. A. Boman, B. Wahlin and R. B. Merrifield (1989). Antibacterial and antimalarial

properties of peptides that are cecropin–melittin hybrids. *FEBS Lett. 259*, 103–106.

20. P. V. Hofsten, I. Faye, K. Kockum, J-Y. Lee, K. G. Xanthopoulos, I. A. Boman, H. G. Boman, A. Engstrom, D. Andreu and R. B. Merrifield (1985). Molecular cloning, cDNA sequencing and chemical synthesis of cecropin B from *Hyalophora cecropia. Proc. Natl. Acad. Sci. USA 82*, 2240–2243.
21. J. Fink, A. Boman, H. G. Boman and R. B. Merrifield (1989). Design, synthesis and antibacterial activity of cecropin-like model peptides. *Int. J. Peptide Protein Res. 33*, 412–421.
22. R. B. Merrifield, P. Juvvadi, D. Andreu, J. Ubach, A. Boman and H. G. Boman (1995). Retro and retroenantio analogs of cecropin–melittin hybrids. *Proc. Natl. Acad. Sci. USA 92*, 3449–3453.
23. D. Andreu, J. Ubach, A. Boman, B. Wahlin, D. Wade, R. B. Merrifield and H. G. Boman (1992). Shortened cecropin A–melittin hybrids: Significant size reduction retains potent antibiotic activity. *FEBS Lett. 296*, 190–194.
24. R. B. Merrifield, D. Andreu, H. G. Boman and H. Steiner in: *Progress in Bioorganic Chemistry and Molecular Biology*, Yu. A. Ovshinnikov, Ed., p. 101–108, Elsevier, Amsterdam 1984.
25. R. B. Merrifield (1963). Solid phase peptide synthesis. I. The synthesis of a tetrapeptide. *J. Am. Chem. Soc. 85*, 2149–2154.
26. G. R. Matseuda and J. M. Stewart (1981). A *p*-methylbenzhydrylamine resin for improved solid-phase synthesis of peptide amides. *Peptides 2*, 45–50.
27. V. K. Sarin, S. B. H. Kent, J. P. Tam and R. B. Merrifield (1981). Quantitative monitoring of solid-phase peptide synthesis by the ninhydrin reaction. *Anal. Biochem. 117*, 147–157.
28. J. P. Tam, W. F. Heath and R. B. Merrifield (1983). S_N2 deprotection of synthetic peptides with a low concentration of HF in dimethyl sulfide: Evidence and application in peptide synthesis. *J. Am. Chem. Soc. 105*, 6442–6455.
29. F. C. Westall, J. Scotchler and A. B. Robinson (1972). The use of propionic acid–hydrochloric acid hydrolysis in Merrifield solid-phase synthesis. *J. Org. Chem. 37*, 3363–3365.
30. S. K. Chowdhury, V. Katta and B. T. Chait (1990). An electrospray-ionization mass spectrometer with new features. *Rapid Commun. Mass Spectrometery 4*, 81–87.
31. D. Hultmark, A. Engstrom, H. Bennich, R. Kapur and H. G. Boman (1982). Insect immunity: Isolation and structure of cecropin D and four minor components from *Cecropia pupae. Eur. J. Biochem. 127*, 207–217.
32. D. Hultmark, A. Engstrom, K. Andersson, H. Steiner, H. Bennich and H. G. Boman (1983). Insect immunity. Attacins, a family of antibacterial proteins from *Hyalophora cecropia. EMBO J. 2*, 571–576.
33. Y.-H. Chen, J. T. Yang and K. H. Chau (1974). Determination of the helix and beta form of proteins in aqueous solution by circular dichroism. *Biochemistry 13*, 3350–3359.
34. C. M. Drain, B. Christensen and D. Mauzerall (1989). Photogating of ionic currents across a lipid bilayer. *Proc. Natl. Acad. Sci. USA 86*, 6959–6962.
35. P. Mueller, D. O. Rudin, H. T. Tien and W. C. Wescott (1963). Reconstitution of excitable cell membrane structure *in vitro* circulation. *J. Phys. Chem. 67*, 534–535.
36. M. Montal and P. Mueller (1972). Formation of biomolecular membranes from lipid monolayers and a study of their electrical properties. *Proc. Natl. Acad. Sci. USA 69*, 3561–3566.
37. R. Fettiplace, D. M. Andrews and D. A. Haydon (1971). The thickness, composition and structure of some lipid bilayers and natural membranes. *J. Membr. Biol. 5*, 277–296.
38. O. D. Monera, T. J. Sereda, N. E. Zhou, C. M. Kayt and R. S. Hodges (1995). Relationship of side-chain hydrophobicity and α-helical propensity on the stability of the single-stranded amphipathic α-helix. *J. Peptide Science 1*, 319–329.
39. R. V. Wolfenden, P. M. Cullis and C. C. Southgate (1979). Water, protein folding and genetic code. *Science 206*, 575–577.
40. C. Chothia (1976). The nature of the accessible and buried surfaces in proteins. *J. Mol. Biol. 105*, 1–14.
41. D. Wade, A. Boman, B. Wahlin, C. M. Drain, D. Andreu, H. G. Boman and R. B. Merrifield (1990). All-D amino acid-containing channel-forming antibiotic peptides. *Proc. Natl. Acad. Sci. USA 87*, 4761–4765.
42. E. L. Merrifield, S. A. Mitchell, J. Ubach, H. G. Boman, D. Andreu and R. B. Merrifield (1995). D-enantiomers of 15-residue cecropin A-melittin hybrids. *Int. J. Peptide Protein Res. 46*, 214–220.
43. F. Jahnig (1983). Thermodynamics and kinetics of protein incorporation into membranes. *Proc. Natl. Acad. Sci, USA 80*, 3691–3695.
44. M. K. Mathew and P. Balaram (1983). A helix dipole model for alamethicin and related transmembrane channels. *FEBS Lett. 157*, 1–5.
45. P. Schoch and D. F. Sargent (1980). Quantitative analysis of the binding of melittin to planar lipid bilayers allowing for the discrete-charge effect. *Biochim Biophys. Acta 602*, 234–247.
46. R. Latorre and O. Alvarez (1981). Voltage-dependent channels in planar lipid bilayer membranes. *Physiol Rev. 61*, 77–150.
47. G. Menestrina, K.-P. Voges, G. Jung and G. Boheim (1986). Voltage-dependent channel formation by rods of helical polypeptides. *J. Membr. Biol. 93*, 111–132.